Two-step build-up of a thermoreversible polymer network: From early local to late collective dynamics

H. Souguir, O. Ronsin, C. Caroli, and T. Baumberger*

Institut des Nanosciences de Paris (INSP), Université Paris 6, UMR CNRS 7588, 2 place Jussieu, 75005 Paris, France

(Received 20 February 2015; published 10 April 2015)

We probe the mechanisms at work in the build-up of thermoreversible gel networks, with the help of hybrid gelatin gels containing a controlled density of irreversible, covalent crosslinks (CLs), which we quench below the physical gelation temperature. The detailed analysis of the dependence on covalent crosslink density of both the shear modulus and optical activity evolutions with time after quench enables us to identify two stages of the physical gelation process, separated by a temperature-dependent crossover modulus: (i) an early nucleation regime during which rearrangements of the triple-helix CLs play a negligible role, and (ii) a late, logarithmic aging one, which is preserved, though slowed down, in the presence of irreversible CLs. We show that aging is fully controlled by rearrangements and discuss the implication of our results in terms of the switch from an early, local dynamics to a late, cooperative long-range one.

DOI: 10.1103/PhysRevE.91.042305 PACS number(s): 82.70.−y, 61.20.Lc, 61.43.−j, 62.20.F−

I. INTRODUCTION

Disordered solids, namely various glasses, polymeric or not, exhibit, following fast relaxation after quench, a slow, usually quasilogarithmic, mechanical strengthening. This self-decelerating behavior is known as aging. As pointed out by Parker and Normand [1], this specificity of glassy dynamics, commonly assigned to the complexity of the free energy landscape, is shared by another class of materials, namely thermoreversible hydrogels. Indeed, although their polymer content is in general very small (typically a few percent), when they are quenched below the gelation temperature T_g, as crosslinks proliferate beyond percolation, the corresponding topological constraints increasingly decimate the paths of easy relaxation.

While logarithmic aging has been evidenced in numerous gels [2], extensive systematic studies have focused on gelatin ones. Gelatin consists of polypeptide chains which self-assemble, when quenched below $T_g \simeq 30^\circ$C, via partial renaturation of the native collagen triple-helix structure [3,4] from the high temperature free chain coil configuration. The chirality of the resulting crosslinks (CLs) permits one to characterize this gelation dynamics by monitoring the evolution not only of the storage shear modulus G, but also of the optical activity and hence the renatured collagen fraction χ [5].

There is general agreement [2,6] on the fact that gelation proceeds via the following scenario:

(i) formation of triple-helix nuclei whose critical size decreases as temperature T decreases below T_g and

(ii) subsequent extension (growth) of these critical crosslinks while nucleation gradually slows down as the network mesh size decreases.

The associated depletion of the entropy supply of the polymer chains leads to gradual exhaustion of these nucleation and growth processes and, hence, to a severe slowing down of the growth of G. This is often described as "saturation of the modulus," since many authors traditionally resort to the log G versus t plot, an example of which is shown in Fig. 1 (inset). However, in this late regime, as illustrated in Fig. 1,

(iii) structural relaxation does not stop but crosses over to the self-decelerating, logarithmic dynamics ($G \sim \log t$) characteristic of glass aging. No trend toward saturation has been observed up to two months [7].

This aging behavior, specific of physical (as opposed to covalent) gels, has been assigned to network rearrangements taking place via thermally activated zippings and unzippings of the H-bond-stabilized triple helices, i.e., to the thermoreversibility of the CLs. However, no direct information about the relative weight of nucleation and growth versus such "plastic" crosslink rearrangements in the early and late regimes of network build-up has been available up to now. In order to try and shed more light on this issue, we resort in this work to an approach which parallels the study of point-to-set correlations in glass-forming liquids [8]. That is, in order to assess the influence of reversibility on the dynamics, we introduce in the gels a controlled density of covalent CLs.

More precisely, we first form at a temperature above T_g a covalent network, characterized by its shear modulus G_{ch}. Further covalent crosslinking is then inhibited, after which we quench the gel below T_g so as to allow for physical crosslinking to take place. This leads to the formation of "chemical-physical hybrid gels" [9–11], the aging dynamics of which we monitor via the evolution of their modulus $G(t)$ and renatured collagen fraction $\chi(t)$.

As can be intuitively expected, increasing G_{ch}, and hence the fraction of irreversible CLs, results in a slower and slower dynamics. Moreover, the qualitative features of $\chi(t)$ and $G(t)$—including nonsaturating, logarithmic aging of the shear modulus—are fully preserved. Detailed quantitative analysis of the dependence upon G_{ch} of network build-up dynamics enables us to identify a temperature-dependent crossover shear modulus separating (i) an early nucleation regime, during which crosslink rearrangements play a negligible role, from (ii) the late, logarithmic aging one, fully controlled by rearrangements. We discuss the implication of our results in terms of the switch from an early, local dynamics to a late, cooperative long-range one.

*tristan@insp.jussieu.fr

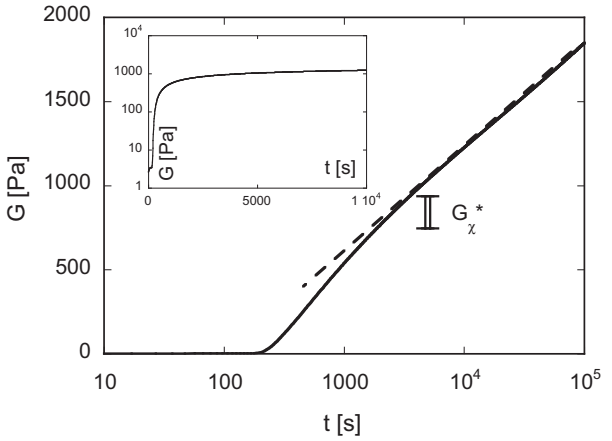

FIG. 1. Evolution of the shear modulus of a 5 wt % gelatin gel in water at $T = 20°$C, vs logarithm of time after quench. The dashed line fits the late aging behavior. The double bar indicates the crossover region as deduced from optical data (see Sec. III A). Inset: same data in the lin-log representation.

II. MATERIALS AND METHODS

Sample preparation. The first stage consists in the preparation of a covalently bonded gelatin network with a given modulus G_{ch}. For this purpose we use an enzymatic route that we have described in detail elsewhere [12].

In short, we dissolve gelatin (300 Bloom, type A from porcine skin, Sigma) in deionized water at 65°C. After total dissolution of the polymer, the solution is quickly mixed at 40°C with a Tgase enzyme solution (microbial transglutaminase, Activa-WM, Ajinomoto Foods Europe SAS) so as to reach a final composition of 5 wt % gelatin and 2.6 nmol of Tgase (corresponding to an enzymatic activity of 2 U). The solution is poured into the measurement cells of both a rheometer and a polarimeter (see below). Gelation then proceeds at $T_{set} = 40°$C. At this temperature, chosen well above $T_g \simeq 30°$C, no triple-helix *reversible* crosslink can form, whereas Tgase catalyzes actively the formation of interchain *covalent* bonds between two specific residues [13].

When the target shear modulus level, as monitored in the rheometer, is reached, the enzyme is inhibited by quickly heating both samples up to 70°C and staying at this temperature for 10 min, after which they are cooled down back to 40°C. We have checked that the shear modulus, measured at this temperature, remains constant over days. The shear moduli of the chemical gels we study here range from 20 to 1600 Pa. The corresponding network mesh sizes, estimated from the scaling relation [14] $\xi \sim (k_B T/G')^{1/3}$, thus range from ∼55 down to ∼15 nm.

The physical gelation is subsequently triggered by quenching to the working temperature $T < T_g$—in most cases, $T = 20°$C.

Shear modulus measurements. The elastic response of the hybrid gel is characterized in a stress-controlled rheometer (AMCR 501, Anton Paar) equipped with a plane-plane, sand-blasted cell, oscillating at 1 Hz, with a 1% strain amplitude so as to operate in the linear response regime. The sample is protected against solvent evaporation by a paraffin oil rim. We quenched the samples at the maximum rate (15 °C/min) permitted by the thermoelectric cooling device so as to minimize the formation of physical crosslinks prior to reaching the target temperature T.

We need to characterize the hybrid gels by the modulus of the purely covalent network at temperature T. Since physical gelation starts without any time lag (see below), it is not possible to measure reliably $G_{ch}(T)$. Since the gel elasticity is of entropic origin, the shear modulus at fixed network structure scales as the absolute temperature T. So, as a proxy for $G_{ch}(T)$, we use the following expression: $G_{ch}(T) = (T/T_{set})G_{ch}(T_{set})$ with both temperatures in degrees Kelvin.

All the gels studied here exhibit a very small level of viscoelastic losses: the ratio G''/G' of the loss to storage moduli at 1 Hz, typically $\lesssim 1 \times 10^{-2}$ at the end of the quench, keeps decreasing as physical gelation proceeds. So, for the sake of simplicity we characterize them by their sole storage shear modulus, noted G.

Optical activity measurements. The rotation angle α of the polarization plane of light passing through a 1-cm gelatin sample is measured using a spectropolarimeter (Jasco 1100) operating at 436 nm. Gelatin is optically active in both the random coil (above T_g) and helix (below T_g) conformations. The renatured collagen fraction χ is obtained as [5,6]

$$\chi = \frac{\alpha - \alpha^{\text{coil}}}{\alpha^{\text{collagen}} - \alpha^{\text{coil}}}, \tag{1}$$

where α^{coil} is the rotation angle measured in the coil state above T_g and extrapolated down to T according to [6], and α^{collagen} is the rotation angle of a 1-cm-thick, 5 wt % collagen sample [5].

The sample cell is thermalized by a water circulating circuit. Quenching is achieved by switching the circulating water between two different temperature-controlled baths. Although the total duration of the quench is comparable to the one achieved in the rheometer, it is impossible to match precisely the shapes of the transients, the initial cooling rate being faster in the polarimeter. In the following we choose the time origin for physical gelation as the instant at which the sample temperature reaches the target value T.

III. RESULTS AND DISCUSSION

Figure 2 shows the time evolution of the shear modulus G and helix fraction χ for values of the modulus of the covalent network at the working temperature $T = 20°$C, increasing from 0 (purely physical gel) to 1480 Pa. The semilogarithmic representation [Fig. 2(a)] reveals that the evolution of G is qualitatively preserved in the presence of covalent CLs. In particular, late quasilogarithmic aging is observed for all values of G_{ch}, with no trend to saturation being observable up to 1×10^5 s.

The early evolution of the modulus is best displayed by plotting the increment $\Delta G = G(t) - G_{ch}$ of its value from that immediately after quench. The most conspicuous feature of the corresponding plot (Fig. 3) consists of the initial behavior of ΔG: while the purely physical gel exhibits a finite delay before the emergence of a measurable modulus, for all hybrid gels, however small $G_{ch} > 0$, the initial rate of growth of ΔG is finite, decreasing as G_{ch} increases. The origin of this

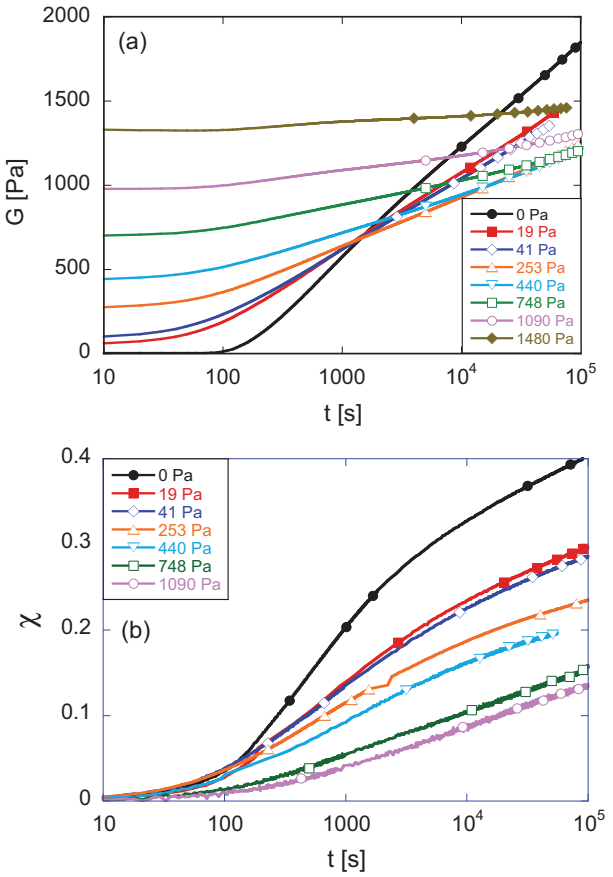

FIG. 2. (Color online) (a) Shear modulus dependence on time after quench to $T = 20^{\circ}$C of a set of hybrid gels with various densities of covalent crosslinks. The labels indicate the values of the shear modulus G_{ch} of the corresponding chemical networks. (b) Evolution of the renatured collagen fraction χ for the same gels. Data from the $G_{ch} = 1480$ Pa gel have been discarded due to the smallness of the corresponding signal-to-noise ratio.

discontinuous behavior is clear: while, in the purely physical gel case, percolation of the triple-helix CL has to be reached for a finite G to emerge, in the presence of a preexisting percolating covalent network, physical CL formation is immediately revealed. This leads us to an important inference: namely, a fraction at least of the triple-helix CLs involve polymer strands belonging to the covalent network. This proves that our hybrid gels *do not* consist (as is the case of "double network" ones [15]) of two interpenetrating but independent networks of different natures—which would contribute additively to G. Finally, the decrease of the initial slope with increasing G_{ch} indicates that covalent interchain bonds do not act as inhomogeneous nucleation centers for triple-helix formation.

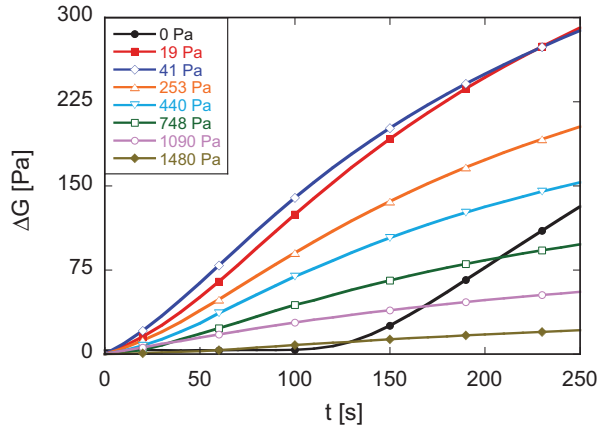

FIG. 3. (Color online) Early evolution of the excess shear modulus $\Delta G(t) = G(t) - G_{ch}$. Same data as in Fig. 2(a).

The evolution of the helix fraction χ is shown in Fig. 2(b). Here again the hindering effect of covalent CLs translates into the gradual slowing down of the dynamics with increasing CL density. Unlike G, the optical activity of the purely physical gel does not exhibit any latency since it is insensitive to the connectivity of the polymer chain system.

Beyond these general remarks we need to define a procedure to compare modulus build-up in our various gels. We choose to proceed as follows: we first measure the time $t_0(G_{ch})$ for which the modulus of the purely physical gel $G_{ph}(t)$ reaches the value G_{ch}; then we shift the $G(t; G_{ch})$ curve of the corresponding hybrid gel by $t_0(G_{ch})$ along the time axis.

The rationale for this choice is the following. A purely physical gel and a chemical one exhibit distinct network topologies, since triple-helix CLs are spatially extended, involving three chains, while the pointlike covalent ones connect two chains only. However, as gel elasticity is of purely entropic origin, G is controlled by the entropy reduction of the polymer chain system due to crosslinking and, hence, is an indicator of the density of degrees of freedom which are frozen at the corresponding stage of gelation [16]. So, our procedure amounts to choosing for the common reference the situation where the density of degrees of freedom which remain available for further evolution for both gels is comparable.

The resulting plot (Fig. 4) exhibits a striking structure. Namely, up to a modulus level $G^{\star}$ lying in the 700–800 Pa range, the hybrid gel data corresponding to $G_{ch} \lesssim G^{\star}$ closely bunch with $G_{ph}(t)$. Beyond this, they separate from G_{ph} and bend sharply into a splayed set of quasi-log-linear curves.

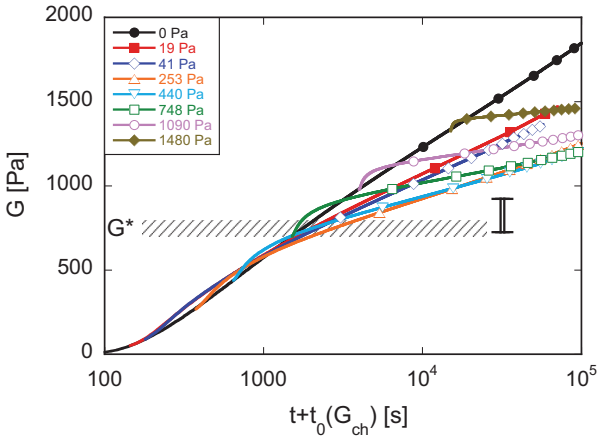

FIG. 4. (Color online) Same data as in Fig. 2(a): each hybrid gel curve has been shifted along the time axis so as to allow comparison with the purely physical gel one $G_{ph}(t)$ (black curve, solid dots). $t_0(G_{ch})$ is the time at which $G_{ph} = G_{ch}$. The hatched strip indicates the end of the early regime. The double vertical bar indicates the crossover range as obtained from $\chi(G)$ data (see Sec. III A).

For $G_{ch} \gtrsim G^\star$, separation occurs for $G - G_{ch}$ values which decreases rapidly with G_{ch}.

This structure leads us to identify, in the network build-up process, two clearly different regimes separated by a crossover:

(i) an early stage in which the dynamics is basically insensitive to the nature of preexisting CLs and

(ii) a late, aging one in which the modulus growth is strongly affected by the degree of CL reversibility as revealed by the marked decrease with increasing G_{ch} of the logarithmic slope.

We now discuss separately in more detail the features of these two regimes.

A. Early stage

The bunching (i.e., quasicollapse) of the G curves (Fig. 4) suggests that, in this regime, it is the total gel modulus which codes the network evolution. If such is the case, other characteristics of the network should exhibit a change of regime at a crossover value comparable to $G^\star$. A natural candidate for checking this proposition is the helix fraction χ which we therefore plot, in the "master curve" representation of Joly-Duhamel *et al.* [17], as a function of G.

Figure 5(a) shows the corresponding plot for a purely physical gel at $T = 20°$C. The finite $\chi(G = 0)$ value measures the helix fraction at percolation. At the modulus value noted $G^\star_\chi = 770 \pm 40$ Pa, $\chi(G)$ crosses over from a linear regime to a markedly sublinear one. The same analysis of the hybrid gel data for G_{ch} values up to 750 Pa reveals, as illustrated in Fig. 5(b), the persistence of a low-G linear regime terminating at $G^\star_\chi(G_{ch})$. We find [see inset of Fig. 5(b)] that $G^\star_\chi$ does not exhibit any significant dependence on G_{ch}. The mean ($\pm$ standard deviation) $\bar{G}^\star_\chi = 830\,(\pm 90)$ Pa is fully compatible with the crossover level $G^\star$ previously identified from the bunching of the $G(t)$ data (see Fig. 4). Moreover, the $G^\star_\chi$ crossover turns out (Fig. 1) to lie very close to the emergence of the logarithmic aging regime. In order to check the robustness of these features with respect to temperature we have performed the same analysis on physical gels of the same composition, quenched at $T = 15$ and 10°C. As is well known, the smaller T, the faster the gelation dynamics. The shape of the $\chi(G)$ curves is preserved while $\bar{G}^\star_\chi$ increases as T decreases—its values, reported in Table I, remaining in the close vicinity of the entry into the log stage (see Fig. 7).

These results bring strong support to our above assumption of the existence of an early regime, the development and termination of which are coded by the total elastic modulus; i.e., they are quasi-insensitive to network topology and crosslink reversibility.

Moreover, the quasilinearity of the early $\chi(G)$ dependence suggests a simple, qualitative interpretation; namely, according to the entropic origin of gel elasticity, it is commonly admitted [14] that, as a first approximation, the shear modulus scales linearly with the CL density. During physical gelation, only triple-helix CLs are formed. So, on the same level of approximation, we may write for the variations of G and χ induced by an increment $\Delta\nu$ of CL density $\Delta G \sim k_B T \Delta\nu$ and $\Delta\chi \sim \bar{\ell}\Delta\nu$ with $\bar{\ell}$ the average triple-helix CL length. From this, $d\chi/dG =$ const immediately translates into the statement

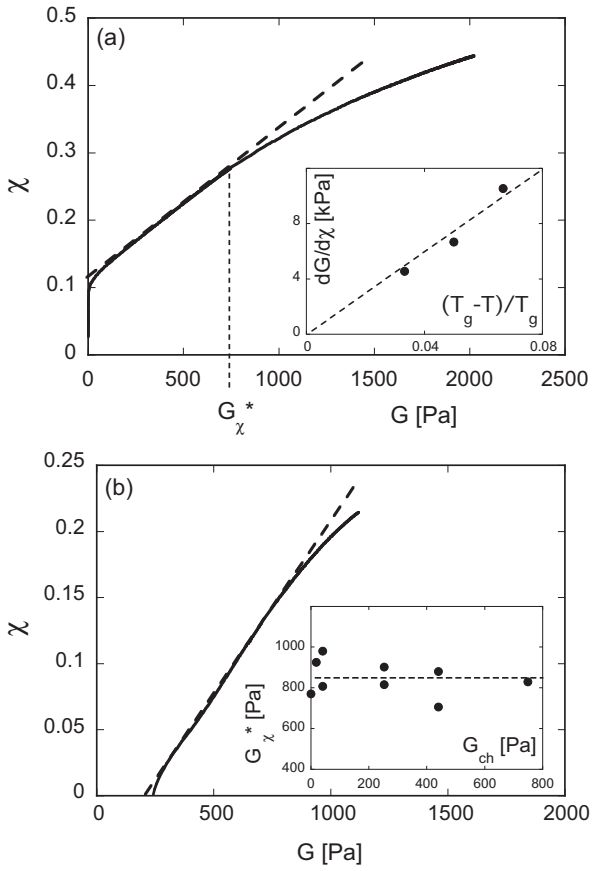

FIG. 5. (a) Helix fraction χ vs shear modulus G for the physical gel at $T = 20°$C. The thick dashed line is the linear fit to the initial regime ending at $G = G^\star_\chi$. Inset: Inverse of the linear regime slope, $dG/d\chi$, vs reduced departure from gelation temperature $T_g = 30°$C. (b) Helix fraction vs shear modulus for a hybrid gel with $G_{ch} = 253$ Pa at $T = 20°$C. Inset: End of linear regime $G^\star_\chi$ vs chemical modulus G_{ch} at the same temperature.

that $\bar{\ell}$ remains stationary over the early gelation regime. Note that this assertion agrees with the conclusion reached by Guo *et al.* [6], who were able to deduce, from the evolution of χ upon remelting physical gels of various ages, the distribution of lengths of these rods at various stages of gelation. They found that it remains quasi-invariant in the corresponding time regime (while $\bar{\ell}$ slowly drifts, at later times, toward larger values).

One step further, in agreement with nucleation theory [18], we can expect the critical nucleus size and, hence, $\bar{\ell}$ to diverge upon approaching the gelation temperature T_g. Since, from our above remarks, $1/\bar{\ell} \sim dG/d\chi$, we have plotted [see inset of Fig. 5(a)] $dG/d\chi$ versus $(T_g - T)/T_g$. We find that our data

TABLE I. Temperature-dependent values of the characteristic moduli $G^\star_\chi$ (see Sec. III A) and $\mathcal{G}$ (see Sec. III B).

T (°C)	$\bar{G}^\star_\chi$ (Pa)	$\mathcal{G}$ (Pa)
10	2650	2016 ± 310
15	1670	1300 ± 160
20	830	685 ± 15

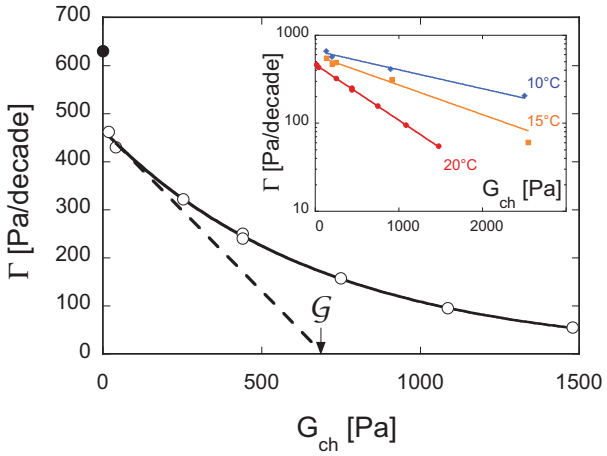

FIG. 6. (Color online) Logarithmic slope $\Gamma = dG/d(\log_{10} t)$ vs G_{ch} for hybrid gels at $T = 20°C$. Solid line: best fit $\Gamma = A \exp(-G_{ch}/\mathcal{G})$ with $\mathcal{G} = 685$ Pa. The purely physical gel data point (solid dot) has been excluded from the fit (see text). Inset: Γ vs G_{ch} at different temperatures below T_g.

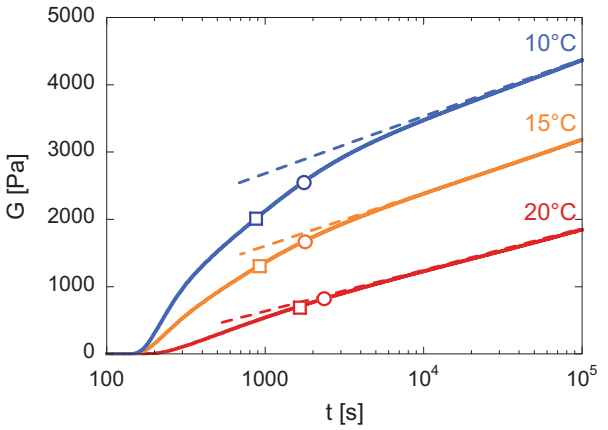

FIG. 7. (Color online) Modulus build-up curves $G_{ph}(t)$ at different temperatures. The circles indicate the crossover modulus $\tilde{G}^{\star}_{\chi}$. The squares indicate the modulus $\mathcal{G}$ characteristic of the sensitivity of gel aging to G_{ch} (see Table I).

for $T = 10$, 15, and 20°C extrapolate linearly to the origin, indicating the expected $(T_g - T)^{-1}$ divergence.

B. Late stage

This regime is characterized by the logarithmic increase with time of the shear modulus which emerges close above the crossover level $G^{\star}$ defined on Fig. 4. As already mentioned, the logarithmic slope

$$\Gamma = \frac{dG}{d(\log_{10} t)} \tag{2}$$

is markedly dependent upon G_{ch}, i.e., on the density of irreversible CLs. Figure 6 displays the values of Γ measured at $T = 20°C$ for various hybrid gels with G_{ch} ranging from 20 to 1480 Pa. These data are very nicely fitted by the expression

$$\Gamma = \Gamma_0 \exp\left[-\frac{G_{ch}}{\mathcal{G}}\right] \tag{3}$$

with $\mathcal{G} = 730 \pm 15$ Pa. Note that the extrapolated slope $\Gamma_0 = 466 \pm 4$ Pa/decade lies noticeably below the value (630 Pa, see black dot in Fig. 6) for the purely physical gel. This is attributable to the fact that, while the physical gel does not contain any irreversible CLs, a hybrid gel with vanishingly small G_{ch} presents the finite density of covalent CLs corresponding to the percolation threshold of the chemical network. The above exponential decay is robust with respect to temperature variations as shown in the inset of Fig. 6, which reports data obtained at $T = 10°C$ and 15°C.

This behavior brings to light the existence of a characteristic modulus $\mathcal{G}(T)$ associated with logarithmic aging. We notice that its variation with T parallels that of the crossover modulus while its values remain systematically smaller than $G^{\star}_{\chi}$ (see Table I and Fig. 7).

C. Discussion

These results demonstrate the existence of two dynamical regimes during the build-up of the physical network, which can be clearly differentiated according to their sensitivity to the nature of crosslinks.

While covalent CLs are irreversible, physical ones undergo "rearrangements" via elementary, thermally activated zipping or unzipping events through which helix segments may either grow, shrink, or slide by coherent zipping and unzipping at both ends. The clock is set for these fluctuations by the *cis-trans* isomerization of (Pro-Gly-Pro) sequences of amino acid residues [2,19,20]. As the corresponding mean flip time lies in the 10–100 s range at $T \simeq T_g$, we are dealing here with very slow processes. Rearrangements occur via the biasing of fluctuations under the effect of tension forces along the coil segments which connect the CLs.

In the early regime, the evolutions of both the stiffness and the helix fraction are found to be coded by the instantaneous value of the modulus and are essentially insensitive to the presence of covalent bonds. This implies that the time scale for the nucleation of triple helices is small enough for rearrangements to be quasifrozen, hence the insensitivity to the (reversible or not) nature of the CLs.

Of course, the larger G, the shorter the mesh size and, hence, the thinner the entropic supply available for further nucleation, the rate of which thus decreases—so much so that rearrangement dynamics finally takes over. This results in a rather sharp switch, about a crossover modulus $G^{\star}$. The emerging late regime is characterized by the logarithmic growth of $G(t)$ together with a markedly sublinear $\chi(G)$, which indicates that less and less new helix length is required for further stiffening of the network. Moreover, and most important, the aging dynamics dramatically slows down as the density of irreversible CLs increases. All these features are consistent with a dynamics controlled by CL rearrangements.

Loosely speaking we may distinguish between two types of such processes, which we refer to as *local* and *collective*. We define as a local process the length evolution of a triple-helix segment in the frozen environment determined by its nonevolving nearest neighboring CL. Due to the finite, nanometric size of the gel mesh, the relaxation time for such a process is clearly finite. A simple model of the helix-coil transition on a single polymer strand with fixed ends [21]

and with a Fokker-Planck dynamics [22] for the helix length evolution yields a linear dependence of the relaxation time on the number of monomers in the strand [23]. Explaining the late dynamics by the "local" growth of triple helices nucleated in the early stage would demand a flat distribution of relaxation times spanning more than the three decades over which logarithmic aging has been observed and, hence, a completely unrealistic flat (Gaussian) strand end-to-end distance distribution spanning at least 1.5 decades.

We are therefore led to conclude that the aging behavior results from dynamical interactions between crosslinks, which we call collective processes. More precisely: an elementary (un)zipping event affecting a physical CL induces variations of the tensions of emerging strands; i.e., it acts as a localized force dipole acting on the surrounding elastic medium. This gives rise quasi-instantaneously (i.e., with a delay set by sound propagation) to a power law decreasing strain field which, in turn, modifies the tensions of strands involved in remote CLs, thereby displacing their equilibrium triple-helix length. Due to the long range of elastic couplings, this results in a broadband mechanical noise. As global relaxation, i.e., collagen renaturation, proceeds, one expects that further modulus growth requires cooperation between an increasingly large number of physical CLs and, hence, involves a growing correlated volume and, accordingly, a growing time scale.

In such a picture, introducing an increasing fraction of irreversible CLs has a multiple effect. (i) On the one hand, for a given G it reduces the fraction of rearrangeable CLs. (ii) On the other hand, the average distance between the latter increases, and so does the mechanical noise amplitude. (iii) Moreover, in a purely physical network triple-helix sliding events due to coherent zipping and unzipping at both ends are able to generate an important cooperative effect. Namely sliding of several neighboring triple helices opens the possibility to create local increases of coil strand lengths, thus permitting further helix length variations, even nucleation. Since covalent bonds prohibit helix sliding, such collective effects will certainly be severely hindered by an increasing density of chemical crosslinks. We believe this to play an important part in the exponential decay of the logarithmic aging slope with G_{ch}.

At this stage, pending the development of a theory relating logarithmic aging to definite characteristics of structural evolution, it remains out of the scope of the present work to explain on the basis of these qualitative remarks the observed dependence of the aging dynamics of hybrid gels on their chemical modulus G_{ch}. Progress toward this goal would certainly highly benefit from the development of numerical modeling, possibly in the spirit of the investigations of long time scale glass aging currently developed by several groups [24–26].

This might shed light on an issue of broader interest, also common to glass physics, namely whether or not stiffening during aging is associated with decreasing elastic nonaffinity, i.e., whether slow relaxation drives the system toward gradual homogenization of the internal stresses, as might be suspected on the basis of the following remark. We saw that as time lapses in the late regime, modulus increase involves less and less helix length creation. This is a strong hint of the increasing role played by length-preserving correlated sliding processes, which are destroyed by the interposition of covalent bonds on chains connecting the two helix segments. This topological effect of chemical bonds thus results in the decimation of the possible relaxation paths in configuration space.

ACKNOWLEDGMENTS

We acknowledge funding from the Emergence-UPMC-2010 research program.

[1] A. Parker and V. Normand, Soft Matter **6**, 4916 (2010)
[2] K. te Nijenhuis, *Thermoreversible Networks: Viscoelastic Properties and Structure of Gels*, Advances in Polymer Science Vol. 30 (Springer, New York, 1997), p. 1.
[3] J. D. Ferry, Adv. Protein Chem **4**, 1 (1948).
[4] W. F. Harrington and N. V. Rao, Biochemistry **9**, 3714 (1970)
[5] M. Djabourov and P. Papon, Polymer **24**, 537 (1983).
[6] L. Guo, R. H. Colby, C. P. Lusignan, and A. M. Howe, Macromolecules **36**, 10009 (2003).
[7] V. Normand, S. Muller, J.-C. Ravey, and A. Parker, Macromolecules **33**, 1063 (2000).
[8] L. Berthier and W. Kob, Phys. Rev. E **85**, 011102 (2012).
[9] D. Hellio-Serughetti and M. Djabourov, Langmuir **22**, 8516 (2006).
[10] S. Giraudier, D. Hellio-Serughetti, M. Djabourov, and V. Larreta- Garde, Biomacromolecules **5**, 1662 (2004).
[11] F. Bode, M. Alves da Silva, A. F. Drake, S. B. Ross-Murphy, and C. A. Dreiss, Biomacromolecules **12**, 3741 (2011).
[12] H. Souguir, O. Ronsin, V. Larreta-Garde, T. Narita, C. Caroli, and T. Baumberger, Soft Matter **8**, 3363 (2012).
[13] V. Crescenzi, A. Francescangeli, and A. Taglienti, Biomacromolecules **3**, 1384 (2002).
[14] M. Rubinstein and R. Colby, *Polymer Physics* (Oxford University Press, Oxford, 2003).
[15] J. P. Gong, Soft Matter **6**, 2583 (2010).
[16] J. L. Jones and C. M. Marques, J. Phys. (Paris) **51**, 1113 (1990).
[17] C. Joly-Duhamel, D. Hellio, A. Ajdari, and M. Djabourov, Langmuir **18**, 7158 (2002).
[18] P. J. Flory and E. S. Weaver, J. Am. Chem. Soc. **82**, 4518 (1960).
[19] O. W. McBride and W. F. Harrington, Biochemistry **6**, 1499 (1967).
[20] H. P. Bächinger, P. Bruckner, R. Timpl, D. J. Prockop, and J. Engel, Eur. J. Biochem. **106**, 619 (1980).
[21] S. Kutter and E. M. Terentjev, Eur. Phys. J. E **8**, 539 (2002).
[22] P. G. de Gennes, J. Stat. Phys. **12**, 464 (1975).
[23] C. Caroli (unpublished).
[24] L. K. Béland and N. Mousseau, Phys. Rev. B **88**, 214201 (2013).
[25] N. Mousseau and G. T. Barkema, Phys. Rev. E **57**, 2419 (1998).
[26] Y. Fan, T. Iwashita, and T. Egami, Phys. Rev. E **89**, 062313 (2014).